Latinmag Letters, Volume 3, Special Issue (2013), OD04, 1-8. Proceedings Montevideo, Uruguay

THE IMPORTANCE OF THE COOLING-RATE EFFECT ON MICROWAVE ARCHEOINTENSITY DATA

Wilbor Poletti[1,2], Gelvam A. Hartmann[1], Mimi J. Hill[2], Andrew J. Biggin[2], Ricardo I.F. Trindade[1]

[1] Departamento de Geofísica, Instituto de Astronomia, Geofísica e Ciências Atmosféricas, Universidade de São Paulo

[2] Geomagnetism Laboratory, Department of Earth, Ocean and Ecological Sciences, University of Liverpool, Liverpool, UK.

ABSTRACT

New microwave (MW) palaeointensity data on historical bricks from Northeast Brazil presented a bias towards higher fields when compared to previous double-heating paleointensity estimates; a behavior previously reported for pottery from Southwestern Pacific islands. A simple theoretical approach suggests that the MW bias in both collections is due to a cooling-rate effect on MW estimates. We then experimentally corrected the MW cooling-rate effect on Brazilian fragments, increasing dramatically the degree of consistency between the previous and new results (reducing maximum discrepancies from 25% to 8%). Our results demonstrate the equivalence of microwave and thermal procedures despite the different ways in which the energy is transferred into the spin system (electromagnetic and lattice vibrations). Finally, our results on bricks and ceramics indicate very fast cooling-times after MW steps of less than 1 minute when compared to the several hours cooling in the oven during manucfacture, highlighting the need for systematic cooling-rate corrections to be applied in MW paleointensity studies in the future.

Keywords: paleointensity methods, microwave, cooling-rate correction, Archeomagnetism.

Introduction

Estimates of geomagnetic field intensity prior to 1840 AD rely on accidental records that are far sparser in the southern than in the northern hemisphere. In order to obtain reliable global field models and to understand the morphology of important regional features such as the South Atlantic Magnetic Anomaly, robust paleointensity data from southern latitudes are essential. It is becoming increasingly widely acknowledged among the paleointensity community that the most reliable estimates are those for which differing experimental techniques (*e.g.* thermal and microwave paleointensity methods) produce consistent results.

Different paleointensity methods need to be appropriately corrected in order to rescue concordant final results. It is well known that the differences between cooling times in nature and in the laboratory can influence paleointensity estimations, potentially leading to overestimates of more than 10% for single domain (SD) grains (*e.g.* Fox and Aitken, 1980; Dodson and McClelland-Brown, 1980; Halgedhal *et al.*, 1980; Yu, 2011; Biggin *et al.*, 2013). This influence can be described by a cooling-rate factor used to correct paleointensity estimates, which is expressed by:

$$f_{CR} = (1+\boldsymbol{\Delta} TRM)^{-1} = \left[1 + k \cdot \log_{10}\left(\frac{CT_{natural}}{CT_{laboratory}}\right)\right]^{-1} \quad (01),$$

where $\boldsymbol{\Delta} TRM$ $\boldsymbol{\Delta} TRM$ represents the fraction of paleointensity under- or overestimated, k is a constant which depends on the material properties, and $CT_{natural}$ $CT_{natural}$ and $CT_{laboratory}$ $CT_{laboratory}$ are the cooling times in nature and laboratory, respectively (Dodson and McClelland-Brown, 1980; Halgedhal *et al.*, 1980).

Cooling-rate correction is routinely applied in thermal paleointensity estimates derivatives of Thellier-Thellier (1959) type (TT) and neglected for Triaxe method (TR) (Le Goff and Gallet, 2004; Gallet and Le Goff, 2006). For the microwave paleointensity method (MW) (Walton *et al*., 1992, 1993; Shaw *et al*., 1996), this correction is rarely applied (Shaw *et al*., 1999; Ertepinar *et al*., 2012), and its effectiveness has not yet been fully investigated. Here we strengthen important results from Southwest Pacific (Stark *et al*., 2010) and Northeast Brazil (Hartmann *et al*., 2010) by reconciling microwave paleointensity data with classical double-heating methods to add a sizable new dataset of archeointensity for the southern hemisphere. In doing so, we make a significant methodological advance of relevance to future microwave paleointensity studies.

Materials and methods

We have analyzed archeological brick fragments from Northeast Brazil with ages ranging from 1574 AD to 1910 AD (Hartmann *et al*., 2010). Previous paleointensity estimates for sites Igreja Mem de Sá (IMS), Praça da Sé 1 (SE1) and Museu de Arte Sacra (MAS) were obtained using both TT and TR methods. For sites Museu de Arqueologia e Etnologia (MAE2), Solar Conde dos Arcos (SCA) and Tijoleira Farias (TF), only TT data were obtained. For sites Praça da Sé 2 (SE2), Casa do Pelourinho 27 (CP27), Corpo de Bombeiros (CB) and Galeria Canizares (GC) only TR data are available (Hartmann *et al*., 2010). In all cases the main magnetic carrier is (titano)magnetite with different Ti contents and domain states, as revealed by hysteresis loops, heating and cooling cycles of low-field susceptibility showing a strong decrease at 580 ˚C (Hartman *et al*., 2010). Unblocking temperatures varied between 200 ºC and 475 ˚C for most samples except for fragment MAE2-01 for which the maximum unblocking temperature reaches 550 ˚C. For some samples, hematite and also a high-coercivity, low-unblocking temperature magnetic phase are present (McIntosh *et al*., 2007; 2011), which is probably associated to a substituted hematite phase (Hartmann *et al*., 2010; 2011).

A total of 155 specimens (112 for paleointensity measurements and 43 for cooling-rate correction) from 26 brick fragments corresponding to 10 sites were analyzed using the MW method. An automated microwave system working at a frequency of 14 GHz and coupled to a SQUID magnetometer (Tristan's model DRM 300 rock magnetometer) was used for the experiments (Shaw & Share, 2007). For each fragment, one cylindrical specimen (5 mm diameter x 3 mm long) was first demagnetized with the microwave system, providing an appropriate demagnetization range to perform the paleointensity measurements. Subsequently, a minimum of two sister specimens were selected for MW paleointensity measurements using the Coe (1967) protocol, i.e., the first step in zero-field and the second step in an applied laboratory field. Stepwise magnetization measurements were carried out between 5 W and 40 W with microwave application time intervals varying between 2.5 and 5 s. Each microwave application at a given power for a given time produces a "power-integral" corresponding to a remanence fraction (equivalent to peak temperature in a thermal experiment). Laboratory fields were applied following previous paleointensity results (25-40 μT) (Hartmann *et al*., 2010). Magnetic alteration was monitored through additional steps of microwave partial remanence (pT_MRM) checks (Coe, 1978) and pT_MRM tail checks (Riisager and Riisager, 2001) after every two steps. In addition, domain state bias was evaluated by applying parallel and antiparallel laboratory fields for at least one specimen per fragment. Following insights from modeling and experiments, if parallel and antiparallel estimates yield the same intensity within error, MD bias is likely to be small (Biggin, 2006, 2010). Anisotropy of remanence effects were minimized by applying the magnetic field either parallel or antiparallel to the NRM (Rogers *et al*., 1979; Le Goff and Gallet, 2004).

To be considered valid, an intensity value must have been obtained along the same power-integral interval in which the characteristic magnetic component was isolated (with a MAD ≤ 10˚). We applied strict selection criteria for paleointensity estimates at specimen and fragment level following Hartmann *et al*. (2010; 2011). Arai diagrams (Nagata *et al*., 1963) were computed using a minimum of four temperature steps including at least 40% of the total NRM ($f \geq 0.4$) (Coe, 1978), with standard errors of the slope below 6% of the mean

($\beta \leq 0.06$) (Selkin and Tauxe, 2000). Maximum acceptable pT_MRM checks and pT_MRM tail checks were set at 10% of original NRM for each temperature step. At the fragment level, the estimated standard deviations of all estimations were less than 8% of the mean: this corresponds to a 95% probability of true deviations of less than 15% for n = 2 and above (Paterson *et al*., 2010).

The MW cooling-rate experimental correction used here on the Brazilian brick fragments was based on that developed by Shaw *et al*. (1999), involving two different steps for at least two samples per fragment. Firstly, a laboratory pTRM was imparted in the specimens using a slow cooling time of 25 h from 480 ˚C down to room temperature in an applied laboratory field of 35 μT. Then, we attempted to recover the imparted laboratory field in these specimens using the MW method following exactly the same routine described before for virgin specimens. As a result, up to two cooling-rate correction factors (fMW fMW) per fragment were determined by computing the ratios between the laboratory field (35 μT) and the respective paleointensities recovered by the MW method:

$$fMW = \frac{35}{PI_{CR}} \qquad (02),$$

where PI_{CR} represents the MW paleointensity estimation. The corrected paleointensity (PIC PIC) is given by:

$$PIC = PI.fMW \qquad (03),$$

which is the product between the MW paleointensity measured in virgin specimens (*PI*) and the cooling-rate correction factor (fMW fMW). Finally, an intensity value at fragment level (PI_F PI_F) was computed from the paleointensity average,

$$PI_F = \frac{\sum_{a=1}^{m}[(PIC)_a]}{m} \qquad (04),$$

where *m* represents the number of MW paleointensity results obtained. It is worth noting that we have systematically corrected the parallel or antiparallel induced paleointensity estimates by its respective parallel or antiparallel cooling-rate correction factor.

Results and discussion

From the 155 analyzed specimens (26 fragments), a total of 74 (47 for MW paleointensity and 27 for cooling-rate correction factors) yielded reliable results (see Table 1). The main reasons to reject results were: (a) their low magnetization (< 15 μA/m) due to the small sizes of the specimens, (b) their low percentage of demagnetization (f < 0.4) and (c) magnetic alteration during the experiments evidenced by loss of Arai plot linearity and/or pT_MRM check failure. Magnetic alteration was mainly detected after very unstable microwave absorption, which can be observed by the growth of melt spots in the specimens after stepwise measurements. PT_MRM tail checks were employed to detect non-ideal multidomain-like effects and these produced maximum discrepancies of ~5% in those experiments where the lab-field was aligned antiparallel to the NRM. In parallel experiments where their usefulness is known to be more limited (Biggin & Thomas, 2003; Biggin 2006), the maximum discrepancies were ~ 1.5%. Similarly, when calculating the cooling rate corrected paleointensity at fragment level, results are within 2% if the global average cooling rate factor per fragment is used as opposed to correcting systematically the parallel or antiparallel induced paleointensity estimates by its respective parallel or antiparallel cooling-rate correction factor. All told, these results suggest negligible potential for bias in our palaeointensity results from multidomain-like effects.

Table 1: MW paleointensity estimates.

Site	Age (AD)	n_f/N_f	Fragment	nPI/N	nCR/N	PI_m (µT)	SD (µT)	PI_F (µT)	SD (µT)
MAE2	1557-1591	1/1	MAE2-01	4/11	2/2	37.6	2.1	31.4	1.1
IMS	1561-1591	1/1	IMS-04	4/17	2/2	43.3	1.3	37.2	1.1
SE1	1600-1650	1/1	SE1-193	1/6	2/2				
SE2	1650-1700	1/2	SE2-19	3/6	2/2	44.8	0.8	40.9	2.2
MAS	1666-1686	2/3	MAS-01	3/7	2/2	49.6	0.8	36.4	0.5
			MAS-03	3/6	2/2	48.2	0.7	37.2	1.5
CP27	1675-1725	2/4	CP27-04	4/6	2/2	39.8	0.7	32.2	0.6
			CP27-09	3/7	2/2	49.3	1.2	37.6	1.0
CB	1767-1777	1/2	CB-02	4/4	2/2	41.7	1.8	32.1	1.2
SCA	1780-1781	2/4	SCA-07	3/5	1/2	39.2	0.6		
			SCA-08	3/5	2/2	38.0	0.6	32.3	1.5
TF	1887	1/3	TF-04	3/10	0/2	31.1	1.5		
GC	1900-1920	3/5	GC-02	3/10	2/2	29.9	0.6	24.5	0.4
			GC-03	3/6	2/2	27.8	2.2	24.6	1.8
			GC-04	3/6	2/2	29.0	0.7	25.6	0.2

n_f/N_f: number of fragments retained by the number of fragments measured; nPI/N: number of retained specimens by the number of analyzed specimens; nCR/N: number of retained specimens after cooling-rate correction by the number of measured specimens; PI_m: fragment-level mean before MW cooling correction; PI_F: fragment-level mean after MW cooling-rate correction; SD: standard deviations. Table extracted from Poletti *et al*. (2013).

Figure 1 shows four typical examples of accepted Arai and orthogonal diagrams from two different fragments. Fragment SE2-19 presents very stable thermal demagnetization behavior and (fig. 1a; Hartmann *et al*., 2010). The MW experiment shows a similar result (fig. 1b), but the NRM fraction used to compute the MW intensity (f = 0.52) is smaller than that of the TT value (f = 0.71) with a **Δ**f of 0.19. This behavior results from the less efficient demagnetization/remagnetization in microwave experiments, and is observed in all samples, with **Δ**f values varying from 0.05 to 0.20. For fragment MAS-03, we compared MW results for two specimens, a virgin one (fig. 1c) and a sister sample into which an artificial pTRM was imparted in the laboratory (fig. 1d). Both specimens presented similar fitting parameters (f, g and q) in Arai diagrams. The specimen MAS-03-c01 provided a paleointensity of 44.9 ± 0.4 µT (fig. 1d), which is significantly different from the field imparted in the laboratory (35 µT) using the conventional oven, demonstrating a potential influence of the MW experimental cooling time on the paleointensity estimate and, consequently, the need for a cooling-rate correction.

We have corrected the cooling-rate effect in two ways: theoretically and experimentally (fig. 2). Figures 2a and 2b show TT-MW data for Southwest Pacific islands and Northeast Brazil, after extrapolating Equation 1 for cooling times between 5 and 90s that represent the range of cooling times after microwave applications. For both collections, this simple theoretical MW-correction produces a better agreement between TT and MW data. Results of the MW cooling-rate experimental correction for Brazilian fragments are shown in Figure 2c against TT and TR data. Before cooling-rate correction, MW results produced values systematically higher (up to 25%) than those obtained with TT and TR methods (Figure 2c). But after cooling-rate correction, the difference between TT-TR-MW methods was reduced from 25% to a maximum of 8%, and in some fragments these differences were eliminated entirely (Figure 2c). At fragment-level, intensity estimates were highly consistent with standard deviations less than 8% of the mean.

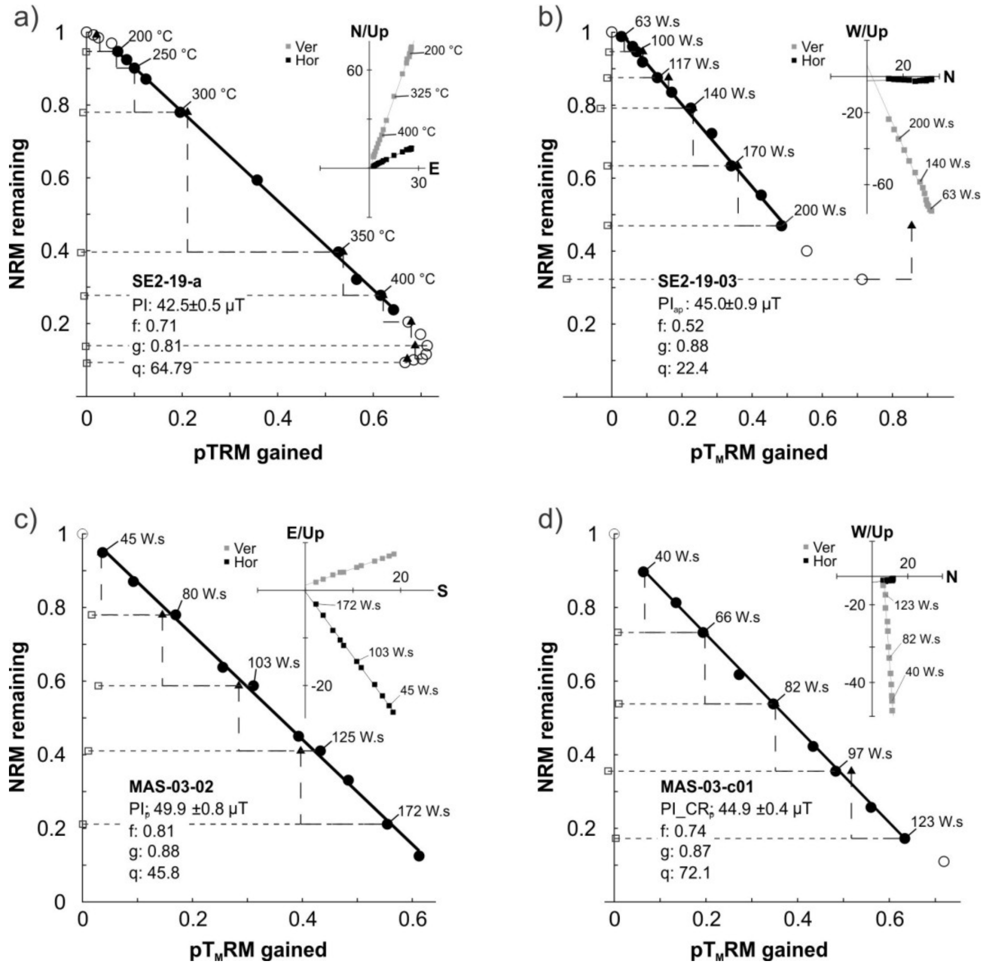

Figure 1. Examples of Arai and orthogonal diagrams for fragments SE2-19 (a-b) and MAS-03 (c-d). In the upper panel, TT (a) and MW (b) results are shown for the same fragment. In the lower panel, results from a virgin specimen (e) and that of a sister sample (f) where a $pT_M RM$ was imparted in the laboratory. In Arai diagrams, circles represent NRM remaining versus pTRM or $pT_M RM$ gained, triangles represent pTRM or $pT_M RM$ checks, and squares represent normalized tail checks. In orthogonal diagrams, gray and black squares represent vertical and horizontal projections, respectively (note samples were not oriented). TT results in (a) are from Hartmann et al. (2010). Figure extracted from Poletti *et al*. (2013).

Finally, we compared the MW cooling-rate experimental correction proposed here with that obtained for TT estimations on Brazilian fragments by Hartmann *et al*. (2010). Firstly, six TT cooling-rate correction factors ($CT_{natural}$ = 25 h; $CT_{laboratory}$ = 30 min) were extrapolated to the shorter time scales of MW treatment using Equation 1. These functions are represented as straight solid lines in Figure 3 which are plotted alongside the corresponding MW cooling-rate experimental correction factors for each fragment (dashed lines in Figure 3). The intersection between straight and dashed lines for each fragment provides an estimate of the laboratory cooling time for MW experiments. For most fragments the MW cooling times are between 5 s and 60 s though two fragments (MAS-03 and IMS-04) have shown cooling times of less than one second (~ 10^{-1} s and ~10^{-2} s, respectively). These differences are likely to be indicative of differing amounts of absorption from the magnetic and electric components of the microwave field (*cf*. Suttie *et al*., 2010). Nevertheless, the comparisons suggest that for this sample set (a) TT and MW cooling-rate corrections have similar experimental behavior, despite the different ways of transferring energy into the spin system (lattice vibrations and electromagnetic), and (b) the different cooling times between natural and laboratory conditions is a significant source of bias in the MW estimates.

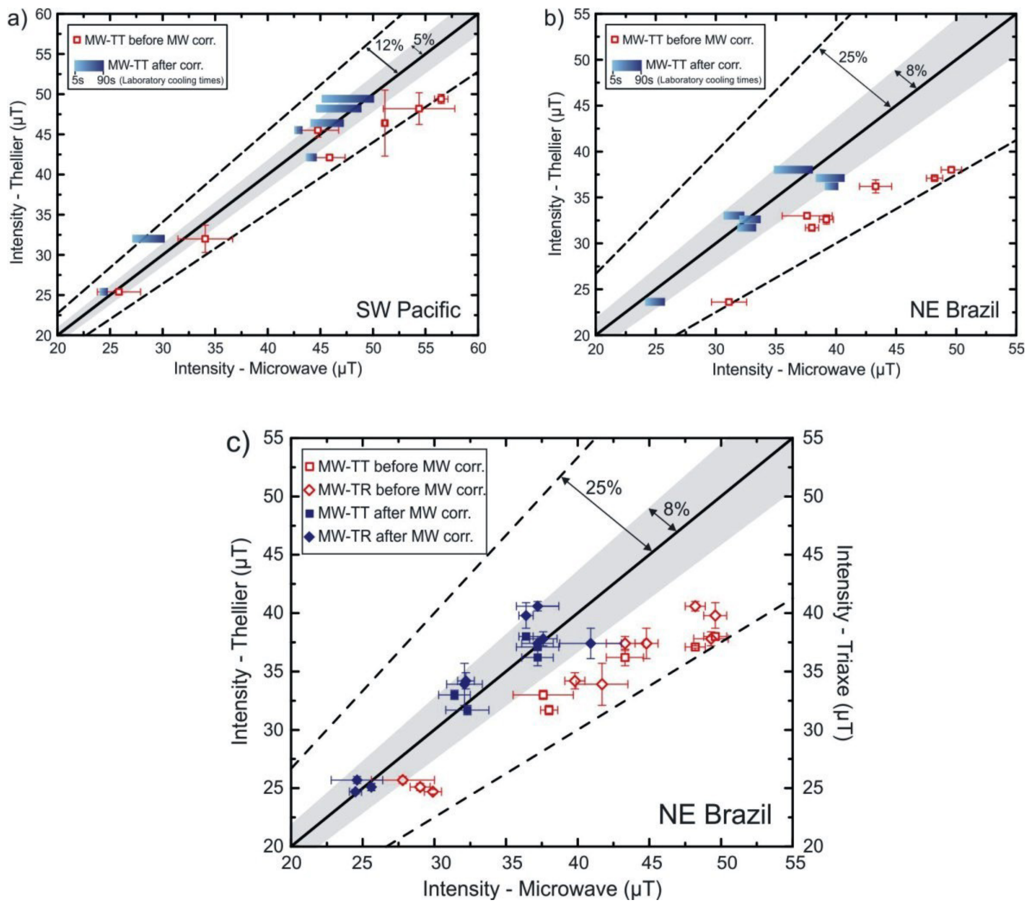

Figure 2. Comparison of intensity results between Microwave (MW) and double-heating methods (TT and TR) based on theoretical (a and b) and experimental (c) approaches. Results are shown before (red open symbols) and after (colored bars and solid blue symbols) MW cooling-rate correction for: (a) SW Pacific islands pottery (MW and TT data from Stark *et al*., 2010), (b and c) NE Brazil bricks (TT and TR data from Hartmann *et al*., 2010). MW data in (b) and (c) were obtained in this study. Dashed lines indicate the area within ± 12% (a) and ± 25% (b and c) and light gray area indicates the area within ± 5% (a) and ± 8% (b and c). Figure extracted and modified from Poletti *et al*. (2013).

Conclusions

The TT-TR-MW experiments and corrections reported here indicate that all three methods can reliably be employed to obtain the past strength of the Earth's magnetic field intensity in baked clay materials. Together they confirm the geomagnetic intensity decay in northeast Brazil presented by Hartmann *et al*. (2010) and improve the estimates presented by Stark *et al*. (2010). Several studies have demonstrated that a cooling-rate correction is needed for the TT method but is not necessary for the TR method. By comparing TT-TR-MW methods we show that the cooling-rate effect could significantly affect MW paleointensity estimates in baked clay materials by up to 25%. However, this effect can be accounted for by applying a simple experimental correction, which relies on paleointensity measurements for sister samples with an imparted TRM. After applying the cooling-rate correction, multi-method paleointensity estimates agreed to within ± 8%. This study has thus demonstrated, for these samples, the need to perform cooling-rate corrections during MW paleointensity acquisitions and suggests that this influence, underrated in previous studies, should be investigated for other materials too.

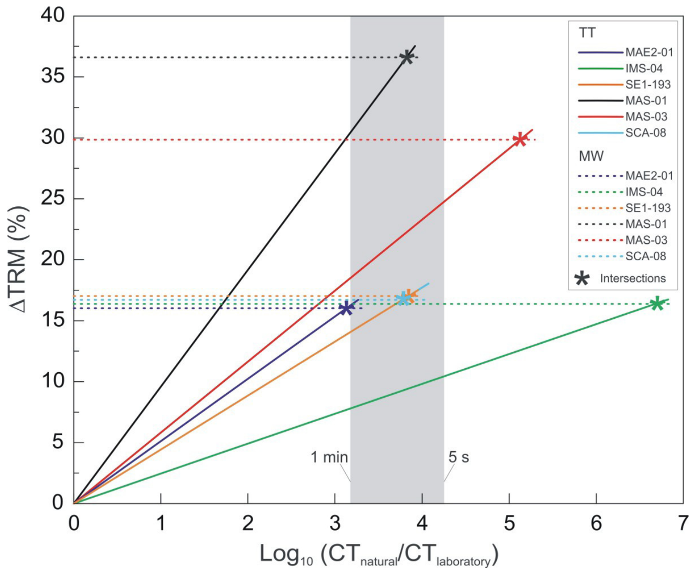

Figure 3. Comparison between the TT and MW cooling-rate factors for six fragments. Straight lines represent TT cooling-rate factors obtained by Hartmann *et al*. (2010a), extrapolated using Equation 1 ($CT_{natural}$ = 25h; $CT_{laboratory}$ = 30min), and plotted as ΔTRM (in %) versus $\log_{10}(CT_{natural}/CT_{laboratory})$. Dashed lines represent the average of fMW per fragment converted to ΔTRM (in %). Stars represent the intersection between extrapolated TT cooling-rate factors and MW cooling-rate factors for the same fragments. The gray area represents the cooling time expected for MW heating steps (5s to 90s). Figure extracted from Poletti *et al*. (2013).

References

Biggin, A. J., 2006. First-order symmetry of weak-field partial thermoremanence in multi-domain (MD) ferromagnetic grains: 2. Implications for Thellier-type palaeointensity determination. *Earth Planet. Sci. Lett., 245*, 454-470. doi: 10.1016/j.epsl.2006.02.034

Biggin, A. J., 2010. Are systematic differences between thermal and microwave Thellier-type palaeointensity estimates a consequence of multidomain bias in the thermal results? *Phys. Earth Planet. Int. 180*, 16-40.

Biggin, A. J., Badejo, S., Hodgson, E., Muxworthy, A., Shaw, J., Dekkers, M., 2013. The effect of cooling-rate on the intensity of thermoremanent magnetization (TRM) acquired by assemblages of pseudo-single domain, multi domain, and interacting single domain grains. *Geophys. J. Int.*, In press.

Biggin, A. J., Thomas, D. N., 2003. The application of acceptance criteria to results of Thellier palaeointensity experiments performed on samples with pseudosingle-domain-like characteristics. *Phys. Earth Planet. Int. 138 (3–4)*, 279–287.

Coe, R. S., 1967. The determination of paleo-intensities of the Earth's magnetic field with emphasis on mechanisms which could cause non-ideal behavior in Thelier's method. *J. Geomag. Geoelectric., 19*, 157-179.

Coe, R. S., Grommé, C. S., Mankinen, E. A., 1978. Geomagnetic paleointensities from radiocarbon dated lava flows on Hawaii and the question of the Pacific non-dipole low. *J. Geophys. Res., 83*, 1740-1756.

Dodson, M., McClelland-Brown, E., 1980. Magnetic blocking temperatures of single-domain grains during slow cooling. *J. Geophys. Res., 85*, 2625-2637. doi: 10.1029/JB085iB05p02625

Ertepinar, P., Langereis, C. G., Biggin, A. J., Frangipane, M., Matney, T., Ökse, T., Engin, A., 2012. Archaeomagnetic study of five mounds from Upper Mesopotamia between 2500 and 700 BCE: Further evidence for an extremely strong geomagnetic field ca. 3000 years ago. *Earth Planet. Sci. Lett.*, 357-358, 84-98. doi: 10.1016/j.epsl.2012.08.039

Fox, J. M. W., Aitken, M. J., 1980. Cooling-rate dependence of thermoremanent magnetization, *Nature, 283*, 462-463. doi:10.1038/283462a0

Gallet, Y., Le Goff, M., 2006. High-temperature archeointensity measurements from Mesopotamia. *Earth Planet. Sci. Lett. 241*, 159-173. doi: 10.1016/j.epsl.2005.09.058.

Halgedahl, S., Day, R., Fuller, M., 1980. The effect of the cooling-rate on the intensity of weak field TRM in single domain magnetite. *J. Geophys. Res*., 85, 3690-3698. doi: 10.1029/JB085iB07p03690

Hartmann, G. A, Genevey, A., Gallet, Y., Trindade, R. I. F., Le Goff, M., Najjar, R., Etchevarne, C., Afonso, M. C., 2011. New historical archeointensity data from Brazil: Evidence for a large regional non-dipole field contribution over the past few centuries. *Earth Planet. Sci. Lett*., 306, 66-76. doi: 10.1016/j.epsl.2011.03.030

Hartmann, G. A., Genevey, A., Gallet, Y., Trindade, R. I. F., Etchevarne, C., Le Goff, M., Afonso, M. C., 2010. Archeointensity in Northeast Brazil over the past five centuries. *Earth Planet. Sci. Lett*., 296, 340-352. doi: 10.1016/j.epsl.2010.05.016

Le Goff, M., Gallet, Y., 2004. A new three-axis vibrating sample magnetometer for continuous high-temperature magnetization measurements: applications to paleo- and archeo-intensity determinations. Earth *Planet. Sci. Lett., 229*, 31-43. doi: 10.1016/j.epsl.2004.10.025

McIntosh, G., Kovacheva, M., Catanzariti, G., Donadini, F., Osete, M. L., 2011. High coercivity remanence in baked clay materials used in archeomagnetism. *Geochem. Geophys. Geosyst*., Q02003, doi: 10.1029/2010GC003310

McIntosh, G., Kovacheva, M., Catanzariti, G., Osete, M. L., Casas, L., 2007. Widespread occurence of a novel high coercivity, thermally stable, low unblocking temperature magnetic phase in heated archeological material. *Geophys. Res. Lett*., 34, L21302. doi: 10.1029/2007GL031168

Nagata, T., Arai, Y., Momose, K., 1963. Secular variation of the geomagnetic total force during the last 5000 years. *J. Geophys. Res*., 68, 5277-5281.

Paterson, G. A., Heslop, D., Muxworthy, A. R. 2010. Deriving confidence in paleointensity estimates. G-cubed 11, Q07z18, Doi 10.1029/2010gc003071.

Poletti, W., Hartmann, G. A., Hill, M. J., Biggin, A. J., Trindade, R. I. F., 2013. The cooling-rate effect on archeointensity estimates. *Geophys. Res. Lett*. In press.

Riisager, P., Riisager, J., 2001. Detecting multidomain magnetic grains in Thellier paleointensity experiments. *Phys. Earth planet. Inter*., 125, 111-117. doi: 10.1016/S0031- 9201(01)00236-9

Rogers, J., Fox, J., Aitken, M. J., 1979. Magnetic anisotropy in ancient pottery, *Nature, 277*, 644-646. doi: 10.1038/277644a0

Selkin, P. A., Gee, J.S., Tauxe, L., Meurer, W. P., Newell, A.J., 2000. The effect of remanence anisotropy on paleointensity estimates: a case study from the Archean Stillwater Complex. *Earth Planet. Sci. Lett*., 245, 454-470. doi: 10.1016/j.epsl.2006.02.034

Shaw, J., and Share, J. A., 2007. A new automated microwave demagnetiser/remagnetiser system for palaeointensity studies, Eos Trans. AGU, Fall Meet. Suppl., 88(52), Abstract, GP53C–1371.

Shaw, J., Walton, D., Yang, S., Rolph, T. C. & Share, J.A., 1996. Microwave archaeointensities from Peruvian ceramics. *Geophys. J. Int*., 124, 241-244. doi: 10.1111/j.1365-246X.1996.tb06367.x

Shaw, J., Yang, S., Rolph, T. C., Sun, F. Y., 1999. A comparison of archaeointensity results from Chinese ceramics using microwave and conventional Thellier's and Shaw's methods. *Geophys. J. Int*., 136, 714-718. doi: 10.1046/j.1365-246x.1999.00765.x

Stark, F., Cassidy, J., Hill, M. J., Shaw, J., Sheppard, P., 2010. Establishing a first archaeointensity record for the SW Pacific, *Earth Planet. Sci. Lett*., 298, 113-124.

Suttie, N., Shaw, J., Hill, M. J., 2010. Direct demonstration of microwave demagnetization of a whole rock sample with minimal heating, *Earth Planet. Sci. Lett*., 292, 357-362.

Thellier, E., Thellier, O., 1959. Sur l'intensité du champ magnetiqué terrestre dans le passé historique et géologique. *Ann. Geophys., 15*, 285-376.

using magnetically anisotropic bricks and tiles, Arch. Sci., 37, 359-373.

Walton, D., Share, J., Rolph, T. C., Shaw, J., 1993. Microwave magnetization. *Geophys. Res. Letters., 20*, 109-111.

Walton, D., Shaw, J., Share, J., Hakes, J., 1992. Microwave demagnetization. *J. Applied Phys., 71*, 1549-1551. doi: 10.1063/1.351230

Yu, Y., 2011. Importance of cooling-rate dependence of thermoremanence in paleointensity determination. *J. Geophys. Res*., 116, B09101. doi: 10.1029/2011JB